were induced, the test was repeated with the same current level intensity or at a current level 1 mA lower.

During the removal of tumors within 3 cm of the pyramidal tracts using intraoperative neuronavigation, subcortical electrical stimulations were carried out repetitively. Bipolar stimulation of five trains with monophasic square waves and a duration of 0.2 msec were applied with a frequency of 1 Hz. For language and sensory testing, a 50-Hz electrical current was delivered.[20] Language functions were assessed during spontaneous speech, naming, reading a paragraph, and were also based on reading comprehension.[20] Sensory function of both positive and negative symptoms was evaluated by the examiner.

We confirmed the points of stimulation by visualization on the neuronavigation system. In all patients, the minimum distances between the points of stimulation and the fiber tracking of the pyramidal tracts were measured with 3D MR imaging during intraoperative neuronavigation.

Surgical Procedures

All of the patients underwent tumor removal with the combined use of tractography-integrated functional neuronavigation and direct fiber stimulation. After the administration of local anesthetic agent, motor function of the four extremities in 28 patients was continuously monitored using the muscle maneuver test[7] during removal of tumors near the pyramidal tracts. In these patients, language function was evaluated with the same testing procedures as those used for electrical stimulation, depending on the location of the tumor. Single-digit multiplication was performed by three patients in whom part of the tumor extended to the left parietal lobe. Resection of the lesions was ceased when a subcortical stimulation elicited an MEP response or language dysfunction. All elicited responses were recorded on video and later confirmed.

Results

Motor function was preserved postoperatively in all patients. In five patients with preoperative mild motor weakness in the upper or lower extremities, motor ability improved to full strength on the 2nd postoperative day (Table 2). Three resections were terminated due to the appearance of a disturbance in reading and naming ability caused by electrical stimulation.

Among 21 patients in whom MEPs were elicited, the distance between the estimated pyramidal tracts and the site of the positive MEPs was 1 cm or less in 18 patients (Fig. 1). Mild preoperative motor weakness in the upper extremities improved intraoperatively in two of four patients overall. Mild and transient motor weakness of the contralateral hand occurred when the first MEP was observed in the other two patients.

The distance between the estimated pyramidal tracts and the site of stimulation was 1 to 2 cm in 15 patients, and MEP recordings were negative in 12 of these patients. Two of these 15 patients suffered postoperative supplementary motor area syndrome,[10] which lasted for 2 weeks. In the remaining five patients, MEPs were never elicited by stimuli more than 2 cm from the estimated pyramidal tracts.

Discussion

This study showed the clinical impact of integrated functional neuronavigation and subcortical electrical stimulation for preserving motor function while attaining adequate tumor resection. Various methods, including positron emission tomography, functional MR imaging, magnetoencephalography, and electrical stimulation, have been shown to be effective for functional mapping and monitoring to preserve motor function at the cortical level. For better surgical outcomes, DT fiber tractography and/or subcortical electrical stimulation have been used to evaluate both the anatomical and functional condition of the pyramidal tracts. Several limitations to these approaches, however, have not been resolved.

Errors in track trajectories estimated by fiber tracking are

TABLE 2

*Relationships among distance, MEP response, and motor function in 40 patients with brain tumors**

Distance (cm)†	No. of Patients	MEP Recordings (no. of patients)	Preop Motor Weakness (no. of patients)‡	Intraop Change in Motor Function (no. of patients)§	Postop Motor Function Results (no. of patients)‖
0–1	20	positive (18)	present (3)		
			upper, Grade 4/5	improved to Grade 4+/5	improved to Grade 5/5
			upper, Grade 4/5	improved to Grade 4+/5	improved to Grade 5/5
			lower, Grade 4/5	no change	improved to Grade 5/5
			none (15)	no change (8), worsened (2)	no deficits (15)
		negative (2)	none (2)	no change (2)	no deficits (2)
1–2	15	positive (3)	none (3)	no change (3)	no deficits (3)
		negative (12)	present (1)		
			upper, Grade 4/5	no change	improved to Grade 5/5
			none (11)	no change (6)	SMA syndrome (2), no deficits (9)
2–3	5	positive (0)	NA	NA	NA
		negative (5)	present (1)		
			upper, Grade 4/5	no change	improved to Grade 5/5
			none (4)	no change (2)	no deficits (4)

* NA = not available; SMA = supplementary motor area.

† Distance between the electrically stimulated white matter and the pyramidal tracts on intraoperative neuronavigation.

‡ Motor function graded according to the Dejong scale.

§ Intraoperative change in motor function is the change in clinical symptoms during awake surgery (in 28 patients) caused by tumor resection, not by electrical stimulation.

‖ Postoperative motor function was compared with preoperative motor function on the 2nd day after the operation.

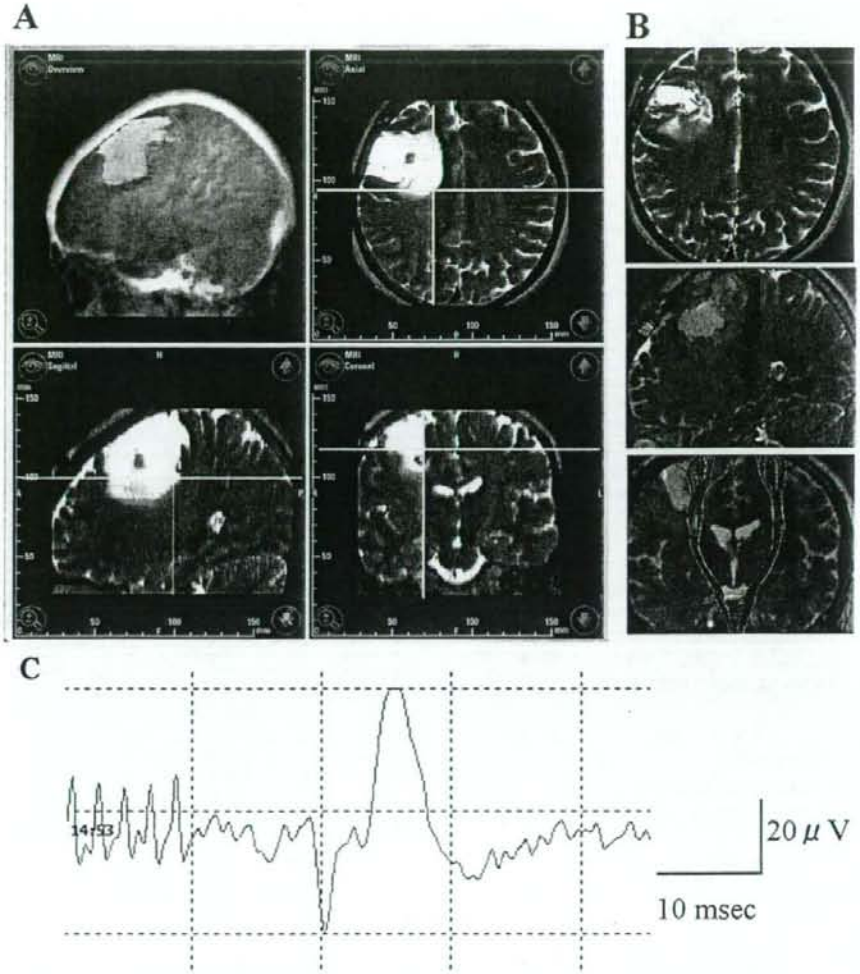

FIG. 1. Subcortical MEPs elicited intraoperatively in a 36-year-old woman with a right frontal diffuse astrocytoma. Her neurological examination was normal preoperatively. A: Intraoperative T_2-weighted MR images showing a hyperintense area (yellow area in *upper left panel*) close to the pyramidal tract identified by fiber tracking (green). During the removal of the tumor, subcortical stimulation elicited MEPs at the bottom of the tumor (intersection of *yellow lines*) 8 mm from the edge of the estimated pyramidal tract. No further removal was performed to avoid causing neurological deficits. B: Postoperative MR images demonstrating that the pyramidal tracts identified by fiber tracking (red) are preserved. C: A typical waveform of MEP response elicited from the left biceps muscle by subcortical stimulation during tumor removal.

known to be caused by low signal-to-noise ratios, the selection of the seed ROIs, the setting of thresholds for fractional anisotropy, the algorithm used in the procedure, or the effects of crossing fibers.[2,4,18] Intraoperative brain shift during surgery should also be considered.[28] In addition to the technical factors mentioned, other factors such as preoperative motor weakness and tumor-related edema can also affect the results of fiber tracking and MEP responses.[16] Additionally, MEP responses are affected by the condition of electrical stimulation;[13] the type of electrodes;[22] and errors in electrical stimulation due to current spread, electrical conductivity, and resistance.[3,11,27,29] These possible errors in the results of MEP recordings may cause postoperative motor deficits following resection of subcortical lesions near the pyramidal tract.[3,8]

Taking these limitations into consideration, complementary use of fiber tracking and subcortical MEPs in the present study offers clinical anatomical–functional information that aids in the preservation of pyramidal tracts. Combined use of these two methods in the present study has shown better surgical outcome in the preservation of motor function than outcomes repeated following MEP monitoring alone[3,8,15] or fiber tracking alone.[1,32] From the neurooncological point of view, subcortical electrical mapping has sig-

nificantly improved the survival rate of patients undergoing low-grade glioma resections.[8] We believe that combined functional neuronavigation and subcortical electrical stimulation during removal of nonmalignant gliomas will contribute to further improvement of the survival rate and maintenance of a high quality of life.

Because intraoperative MR imaging frequently cannot be performed during tumor resection, evaluation of the distance between the site of resection and the pyramidal tracts on intraoperative neuronavigation would be important for determining the optimal time to apply subcortical stimulation. During the removal of tumors located approximately 1 cm from the pyramidal tracts in the course of neuronavigation, repetitive subcortical electrical stimulation should be applied. The presence of subcortical MEPs during resection of a tumor is an important warning sign of the occurrence of permanent motor weakness, and therefore further resection after obtaining the first MEP response should be avoided.[15,16] Alternatively, lesions could be removed without injury to the pyramidal tracts if the estimated fibers were more than 2 cm away on intraoperative neuronavigation. To clarify the critical distance between the subcortex to be electrically stimulated and the estimated pyramidal tracts, further studies with DT image processing during the course of surgery with the use of intraoperative MR imaging are needed.[24] In addition to its use in subcortical mapping of the pyramidal tracts, MEP monitoring using cortical or transcranial electrical stimulation should also be considered as a way to preserve motor function.[17,23,32,33]

Conclusions

In 40 patients with brain tumors located near the pyramidal tracts, MEPs were elicited from the subcortex in 18 of 20 patients when the distance between the stimulated subcortex and the estimated pyramidal tracts on tractography-integrated intraoperative neuronavigation was within 1 cm. In the other 20 patients, with distances greater than 1 cm between the stimulated subcortex and the estimated pyramidal tracts, MEPs were elicited in only three patients. During removal of tumors located within 1 cm from the pyramidal tracts on functional neuronavigation, subcortical electrical stimulation should be applied to preserve motor function.

References

1. Beppu T, Inoue T, Kuzu Y, Ogasawara K, Ogawa A, Sasaki M: Utility of three-dimensional anisotropy contrast magnetic resonance axonography for determining condition of the pyramidal tract in glioblastoma patients with hemiparesis. **J Neurooncol 73:** 137–144, 2005
2. Berman JI, Berger MS, Mukherjee P, Henry RG: Diffusion-tensor imaging-guided tracking of fibers of the pyramidal tract combined with intraoperative cortical stimulation mapping in patients with gliomas. **J Neurosurg 101:**66–72, 2004
3. Cedzich C, Taniguchi M, Schafer S, Schramm J: Somatosensory evoked potential phase reversal and direct motor cortex stimulation during surgery in and around the central region. **Neurosurgery 38:**962–970, 1996
4. Clark CA, Barrick TR, Murphy MM, Bell BA: White matter fiber tracking in patients with space-occupying lesions of the brain: a new technique for neurosurgical planning? **Neuroimage 20:** 1601–1608, 2003
5. Coenen VA, Krings T, Axer H, Weidemann J, Kranzlein H, Hans FJ, et al: Intraoperative three-dimensional visualization of the pyramidal tract in a neuronavigation system (PTV) reliably predicts true position of principal motor pathways. **Surg Neurol 60:** 381–390, 2003
6. Coenen VA, Krings T, Mayfrank L, Polin RS, Reinges MH, Thron A, et al: Three-dimensional visualization of the pyramidal tract in a neuronavigation system during brain tumor surgery: first experiences and technical note. **Neurosurgery 49:**86–93, 2001
7. Dejong RN: Case taking and the neurologic examination, in Barker AB (ed): **Clinical Neurology.** New York: Hoeber-Harper, 1955, Vol 1, pp 1–100
8. Duffau H: Lessons from brain mapping in surgery for low-grade glioma: insights into associations between tumor and brain plasticity. **Lancet Neurol 4:**476–486, 2005
9. Duffau H, Gatignol P, Mandonnet E, Peruzzi P, Tzourio-Mazoyer N, Capelle L: New insights into the anatomo-functional connectivity of the semantic system: a study using cortico-subcortical electrostimulations. **Brain 128:**797–810, 2005
10. Duffau H, Lopes M, Denvil D, Capelle L: Delayed onset of the supplementary motor area syndrome after surgical resection of the mesial frontal lobe: a time course study using intraoperative mapping in an awake patient. **Stereotact Funct Neurosurgery 76:** 74–82, 2001
11. Haglund MM, Ojemann GA, Blasdel GG: Optical imaging of bipolar cortical stimulation. **J Neurosurgery 78:**785–793, 1993
12. Hendler T, Pianka P, Sigal M, Kafri M, Ben-Bashat D, Constantini S, et al: Delineating gray and white matter involvement in brain lesions: three-dimensional alignment of functional magnetic resonance and diffusion-tensor imaging. **J Neurosurgery 99:** 1018–1027, 2003
13. Hern JE, Landgren S, Philips CG, Proter R: Selective excitation of corticofugal neurones by surface-anodal stimulation of the baboon's motor cortex. **J Physiol 161:**73–90, 1962
14. Kamada K, Todo T, Masutani Y, Aoki S, Ino K, Takano T, et al: Combined use of tractography-integrated functional neuronavigation and direct fiber stimulation. **J Neurosurg 102:**664–672, 2005
15. Keles GE, Lundin DA, Lamborn KR, Chang EF, Ojemann G, Berger MS: Intraoperative subcortical stimulation mapping for hemispherical perirolandic gliomas located within or adjacent to the descending motor pathways: evaluation of morbidity and assessment of functional outcome in 294 patients. **J Neurosurg 100:** 369–375, 2004
16. Kinoshita M, Yamada K, Hashimoto N, Kato A, Izumoto S, Baba T, et al: Fiber-tracking does not accurately estimate size of fiber bundle in pathological condition: initial neurosurgical experience using neuronavigation and subcortical white matter stimulation. **Neuroimage 25:**424–429, 2005
17. Kombos T, Suess O, Ciklatekerlio O, Brock M: Monitoring of intraoperative motor evoked potentials to increase the safety of surgery in and around the motor cortex. **J Neurosurgery 95:** 608–614, 2001
18. Lin CP, Tseng WY, Cheng HC, Chen JH: Validation of diffusion tensor magnetic resonance axonal fiber imaging with registered manganese-enhanced optic tracts. **Neuroimage 14:**1035–1047, 2001
19. Masutani Y, Aoki S, Abe O, Hayashi N, Otomo K: MR diffusion tensor imaging: recent advance and new techniques for diffusion tensor visualization. **Eur J Radiol 46:**53–66, 2003
20. Mikuni N, Ohara S, Ikeda A, Hayashi N, Nishida N, Taki J, et al: Evidence for a wide distribution of negative motor areas in the perirolandic cortex. **Clin Neurophysiology 117:**33–40, 2006
21. Mori S, van Zijl PC: Fiber tracking: principles and strategies—a technical review. **NMR Biomed 15:**468–480, 2002
22. Nathan SS, Sinha SR, Gordon B, Lesser RP, Thakor NV: Determination of current density distributions generated by electrical stimulation of the human cerebral cortex. **Electroencephalogr Clin Neurophysiology 86:**183–192, 1993

23. Neuloh G, Pechstein U, Cedzich C, Schramm J: Motor evoked potential monitoring with supratentorial surgery. **Neurosurgery 54:**1061–1072, 2004
24. Nimsky C, Grummich P, Sorensen AG, Fahlbusch R, Ganslandt O: Visualization of the pyramidal tract in glioma surgery by integration diffusion tensor imaging in functional neuronavigation. **Zentralbl Neurochir 66:**133–141, 2005
25. Okada T, Miki Y, Fushimi Y, Hanakawa T, Kanagaki M, Yamamoto A, et al: Diffusion-tensor fiber tractography: intraindividual comparison of 3.0-t and 1.5-t MR imaging. **Radiology 238:** 668–678, 2006
26. Okada T, Mikuni N, Miki, Y, Kikuta K, Urayama S, Hanakawa T, et al: Corticospinal tract localization: integration of diffusion-tensor tractography at 3-t MR imaging with intraoperative white matter stimulation mapping—preliminary results. **Radiology 240:** 849–857, 2006
27. Pouratian N, Cannestra AF, Bookheimer SY, Martin NA, Toga AW: Variability of intraoperative electrocortical stimulation mapping parameters across and within individuals. **J Neurosurg 101:** 458–466, 2004
28. Reinges MH, Nguyen HH, Krings T, Hutter BO, Rohde V, Gilsbach JM: Course of brain shift during microsurgical resection of supratentorial cerebral lesions: limits of conventional neuronavigation. **Acta Neurochir (Wien) 146:**369–377, 2004
29. Taniguchi M, Cedzich C, Schramm J: Modification of cortical stimulation for motor evoked potentials under general anesthesia: technical description. **Neurosurgery 32:**219–226, 1993
30. Witwer BP, Moftakhar R, Hasan KM, Deshmukh P, Haughton V, Field A, et al: Diffusion-tensor imaging of white matter tracts in patients with cerebral neoplasm. **J Neurosurgery 97:**568–575, 2002
31. Yamada K, Kizu O, Mori S, Ito H, Nakamura H, Yuen S, et al: Brain fiber tracking with clinically feasible diffusion-tensor MR imaging: initial experience. **Radiology 227:**295–301, 2003
32. Yu CS, Li KC, Xuan Y, Ji XM, Qin W: Diffusion tensor tractography in patients with cerebral tumors: a helpful technique for neurosurgical planning and postoperative assessment. **Eur J Radiol 56:**197–204, 2005
33. Zhou HH, Kelly PJ: Transcranial electrical motor evoked potential monitoring for brain tumor resection. **Neurosurgery 48:** 1075–1081, 2001

Manuscript submitted June 2, 2006.
Accepted November 7, 2006.

Address reprint requests to: Nobuhiro Mikuni, M.D., Ph.D., Department of Neurosurgery, Kyoto University Graduate School of Medicine, 54 kawahara-cho, Shogoin, Sakyo-ku, Kyoto 6068507, Japan. email: mikunin@kuhp.kyoto-u.ac.jp.

Xenobiotica, December 2008; 38(12): 1471–1475

Increased distribution of carboplatin, an anti-cancer agent, to rat brains with the aid of hyperbaric oxygenation

Y. SUZUKI[1,2], K. TANAKA[2], D. NEGHISHI[1], M. SHIMIZU[1], N. MURAYAMA[1], T. HASHIMOTO[2], & H. YAMAZAKI[1]

[1]*Laboratory of Drug Metabolism and Pharmacokinetics, Showa Pharmaceutical University, Machida, Japan and* [2]*St. Marianna University School of Medicine, Kawasaki, Japan*

(*Received 29 May 2008; revised 13 September 2008; accepted 15 September 2008*)

Abstract

1. The distribution of an anti-cancer agent carboplatin to brains was investigated in combination with hyperbaric oxygenation treatment in rats.
2. After intravenous administration of carboplatin ($30\,mg\,kg^{-1}$) to male Wistar rats, elimination curves of plasma drug concentrations plotted against a time of 45 min were not different with or without hyperbaric oxygenation (at 0.20–0.25 MPa for last 20 min) treatments.
3. Carboplatin concentrations of livers, lungs and kidneys in each group were similar at the endpoint of hyperbaric oxygenation treatment.
4. Under these atmosphere conditions (at 0.10 MPa), carboplatin concentration was at an undetectable level in rat brains ($<0.1\,\mu g\,g^{-1}$ tissue, $n=6$). On the contrary, carboplatin was detected in all brains tested at the levels of $0.5\pm0.3\,\mu g\,g^{-1}$ tissue (mean and standard deviation (SD), $n=6$), $0.8\pm0.5\,\mu g\,g^{-1}$ tissue, and $0.4\pm0.2\,\mu g\,g^{-1}$ tissue in combination with hyperbaric oxygenation at 0.20, 0.22, and 0.25 MPa, respectively, at the endpoint of hyperbaric oxygenation treatment.
5. The results suggest that carboplatin could be uptaken into rat brains at the detectable levels by the aid of hyperbaric oxygenation, consistently with the reported findings of enhanced transendothelial permeability and improved clinical efficacy of carboplatin combined hyperbaric oxygenation therapy.

Keywords: *Hyperbaric oxygenation, carboplatin, brain*

Introduction

Carboplatin (*cis*-diammine-1,1-cyclobutanedicarboxylatoplatinum(II)) is a second-generation platinum antineoplastic agent with clinical efficacy including modest activity against brain tumours (Allen et al. 1987). Recently we obtained a high efficacy of carboplatin

Correspondence: Hiroshi Yamazaki, Showa Pharmaceutical University, Laboratory of Drug Metabolism and Pharmacokinetics, Machida, Tokyo 194-8543, Japan. E-mail: hyamazak@ac.shoyaku.ac.jp

ISSN 0049-8254 print/ISSN 1366-5928 online © 2008 Informa UK Ltd.
DOI: 10.1080/00498250802478313

combined with hyperbaric oxygenation therapy on brain tumours at St. Marianna University School of Medicine Hospital (Tanaka et al. 2004, 2005; Yamazaki et al., 2006; Suzuki et al., 2008). Hyperbaric oxygenation therapy has been generally used to treat decompression sickness, a variety of infections, and ischaemic damages (Chougule et al. 1999). Mechanisms for improved clinical efficacy of a variety of medicines with the hyperbaric oxygenation therapy are not generally known, in spite of their importance in clinical practice. Recently, we indicated that hyperbaric oxygenation increased transendothelial permeability of carboplatin as well as doxorubicin, a known P-glycoprotein substrate, in an *in vitro* model with aid of hyperbaric oxygenation (Yamazaki et al. 2008). Under the hyperbaric oxygenation conditions (at 0.2 MPa for the first 10 min), the transendothelial transport of doxorubicin and carboplatin were increased by 1.3–1.8-fold by hyperbaric oxygenation, like the suppressive effects of verapamil on P-glycoprotein function (Yamazaki et al. 2008). To investigate these novel findings in detail, a confirmation of carboplatin distribution to the brain in an animal model *in vivo* with hyperbaric oxygenation would be needed.

In the present study we investigated the distribution of carboplatin to brains in combination with hyperbaric oxygenation treatment in rats. We report herein the increased distribution of carboplatin to rat brains with the aid of hyperbaric oxygenation. Improved clinical efficacy would be expected as one of the consequences of enhanced distribution of anti-cancer agents to brains with hyperbaric oxygenation.

Materials and methods

Chemical

Carboplatin (CAS number 41575-94-4, molecular weight = 371.25, >99% of purity) was obtained from Bristol-Myers (Tokyo, Japan).

Distribution experiments

The present study was approved by the local committee on the care and use of laboratory animals. A total of 24 male Wistar rats (7 weeks old; Japan SLC, Hamamatsu, Japan) were divided into four experimental groups of six. After cannulation of the inferior vena cava with diethylether anaesthetic, rats were intravenously treated with carboplatin (30 mg kg^{-1}) under atmospheric conditions (at 0.10 MPa). In the cases of HBO treatment, each rat was introduced to a hyperbaric oxygen chamber (Barotec Hanyuda, Tokyo, Japan) at 0.20, 0.22 or 0.25 MPa for 20 min (an increase or decrease of atmosphere for 5 min) from 15 min (from the first zero point) after intravenous injection. This time schedule in the present study was set up in one-third scale in actual human cancer therapy by carboplatin combined with hyperbaric oxygenation therapy at St. Marianna University School of Medicine Hospital (Yamazaki et al. 2006).

Pharmacokinetic analysis of carboplatin

Approximately 1 g of liver, lung, kidney or brain obtained from rats was suspended in 10 mM Tris-HCl buffer (pH 7.5) containing 10 mM EDTA and 100 mM KCl and homogenized with a Teflon-pestle homogenizer. An ultra-filtrate (350–500 µl) was prepared

from 1 ml of plasma samples or tissue homogenates by centrifugation in a Centrifree micropartition unit (Amicon, Beverly, MA, USA) at 2000 *g* and 15°C for 20–60 min. The ultra-filtrate samples containing carboplatin were analysed with an analytical NH_2 column using acetonitrile/methanol/5 mM sodium perchlorate buffer (pH 2.4) (75 : 15 : 10, v/v) at 230 nm by the high-performance liquid chromatography system described previously (Yamazaki et al. 2006). The method yielded similar intra-day and inter-day precision and accuracy of <6% with linearly from 0.1 to 80 $\mu g\,ml^{-1}$ and a recovery rate >98% in the presence of rat plasma or brain homogenates as the reported system (Yamazaki et al. 2006). All statistical analyses were carried out with the InStat program (GraphPad Software, San Diego, CA, USA).

Results and discussion

Figure 1 shows the representative elimination profiles following a 30 $mg\,kg^{-1}$ dose of carboplatin given by intravenous administration. Carboplatin concentrations in the plasma were decreased under the pressure of the atmosphere (0.1 MPa; Figure 1A). With hyperbaric oxygenation treatment adopted at 0.20–0.25 MPa for 20 min; carboplatin concentrations under the three oxygenation conditions were decreased in an apparently similar manner as the atmospheric condition. After the hyperbaric oxygenation treatment, mean carboplatin levels in the plasma (especially at 0.20 MPa) were apparently increased but were not significantly different from the atmosphere group at the endpoint of hyperbaric oxygenation treatment (9–13 $\mu g\,ml^{-1}$; Figure 1B).

At the endpoint of hyperbaric oxygenation, the tissue distribution of carboplatin in rats was determined (Figure 2). As shown in Figure 2A, carboplatin concentrations in kidneys (30–50 $\mu g\,g^{-1}$ tissue) were apparently higher than those in livers or lungs (4–19 $\mu g\,g^{-1}$ tissue). With regard to the effects of hyperbaric oxygenation on the distribution of carboplatin, concentrations of carboplatin in livers, lungs or kidneys were not significantly

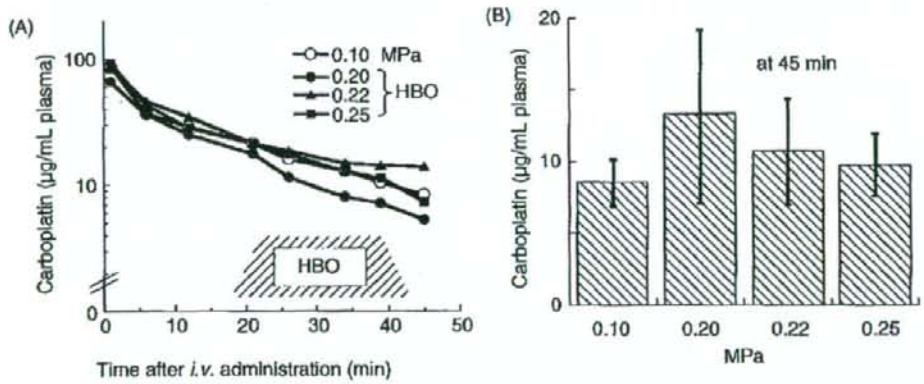

Figure 1. Carboplatin concentrations in plasma as a function of time (A) and at 45 min after intravenous treatment with rats (B). A period of hyperbaric oxygenation treatment was indicated in panel (A) as a hatched bar (increase or decrease of the atmosphere took 5 min). Representative curves were taken from each profile under the atmosphere (at 0.1 MPa) and hyperbaric oxygenation (at 0.20, 0.22, and 0.25 MPa for last 20 min). Data are mean and standard deviation (SD) from six rats in panel (B).

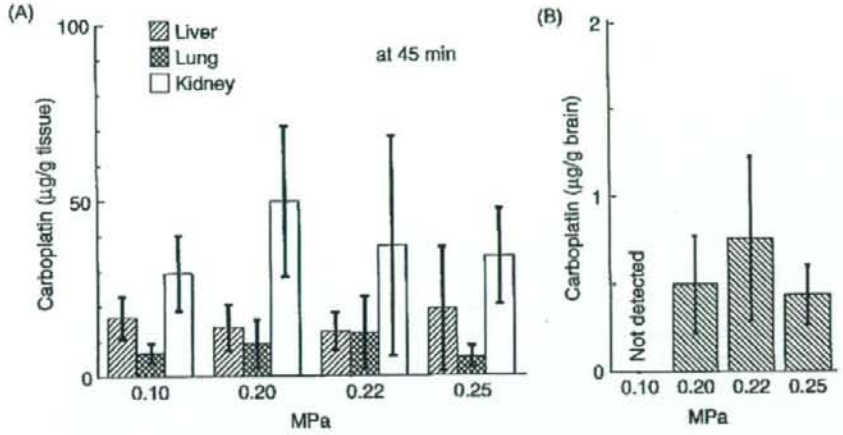

Figure 2. Comparison of carboplarin concentrations in livers, lungs, and kidneys (A) and brains (B) in rats treated with carboplatin ($30\,mg\,kg^{-1}$) and hyperbaric oxygenation (at 0.20–0.25 MPa for last 20 min). Carboplatin concentrations were determined at 45 min after the intravenous treatment.

different among the control atmosphere group (0.1 MPa) and three conditions of hyperbaric oxygenation. On the contrary, carboplatin was detected in all the brains tested in the present study at the levels of $0.5 \pm 0.3\,\mu g\,g^{-1}$ tissue (mean and SD, $n = 6$), $0.8 \pm 0.5\,\mu g\,g^{-1}$ tissue, and $0.4 \pm 0.2\,\mu g\,g^{-1}$ tissue in combination with hyperbaric oxygenation at 0.20, 0.22, and 0.25 MPa, respectively (Figure 2B).

It has been reviewed that a single exposure to hyperbaric or hyperoxic conditions would not seem to affect single-dose pharmacokinetics of drugs eliminated by the kidney (gentamycin) or by the liver with a capacity-limited clearance (pentobarbital, theophylline, caffeine) or with a perfusion-limited clearance (pethidine, lidocaine) (Rump et al. 1999). On the contrary, it could be possible that oxygen-induced cerebral vasoconstriction would result in some modification of drug pharmacokinetics, presumably because of a variety of biochemical changes in the brain such as inactivation of intracellular systems or changes of blood flow rates (Al-Waili and Butler 2007). In the present study, the uptake of carboplatin in rat brain combined with hyperbaric oxygenation was seen (Figure 2B). Mechanisms of carboplatin uptake to the brain had not yet been known. Recently, we have reported that carboplatin had similar endothelial permeability (Yamazaki et al. 2008) compared with doxorubicin or verapamil, which are typical P-glycoprotein substrates (Culot et al. 2008). Increased permeability of P-glycoprotein-dependent carboplatin by hyperbaric oxygenation (like by verapamil) may rapidly reach pharmacologically significant concentrations in the central nervous system. Changes in blood flow derived from oxygen-induced cerebral vasoconstriction could not be ruled out. Although many more factors would also influence clinical efficacy of carboplatin with hyperbaric oxygenation therapy, a possibility of modified biological uptake of carboplatin to the brain by the aid of hyperbaric oxygenation might be relevant to the efficacy with hyperbaric oxygenation therapy for malignant gliomas.

In order to obtain better the distribution of carboplatin to brains, it might be possible to expand the residence time in the hyperbaric oxygenation chamber because the three conditions of oxygenation pressure at 0.20–0.25 MPa gave similar results to

carboplatin pharmacokinetics. However, the present fixed hyperbaric experimental condition came from a simulation at one-third scale to the actual human cancer therapy in our hospital (Yamazaki et al. 2006). Because of rapid elimination of carboplatin in rat plasma (Figure 1), the present analyses were carried out during the combination periods of atmospheric conditions and hyperbaric oxygenation conditions. It might be interesting to calculate pharmacokinetic parameters such as the area under the curve or volume of distribution for carboplatin with more time points. However, the basic conditions were changed in the course of the study with regard to the pressure. It might not allow one to calculate the whole profiles in simple pharmacokinetic analysis. Therefore, we investigated the effects of hyperbaric oxygenation treatments on carboplatin concentrations in plasma and tissues at the endpoint of hyperbaric oxygenation treatment. The further efforts would be necessary to evaluate the hyperbaric oxygen conditions for carboplatin and other medicines to clinical trails in humans.

In conclusion, taken together with the present results and these findings, the increased distribution of carboplatin to rat brain in combination with hyperbaric oxygenation would be consistent with enhanced transendothelial permeability of carboplatin and may support improved clinical efficacy of carboplatin combined with hyperbaric oxygenation therapy.

Acknowledgements

The authors would like to thank Yasuyuki Yoshida, Shintaro Gamura, Haruka Yamaguchi, Rina Tanaka and Moe Kinoshita for their help. This study was supported, in part, by the Ministry of Education, Science, Sports and Culture of Japan, the Ministry of Health, Labor and Welfare of Japan.

References

Allen JC, Walker R, Luks E, Jennings M, Barfoot S, Tan C. 1987. Carboplatin and recurrent childhood brain tumors. Journal of Clinical Oncology 5:459–463.

Al-Waili NS, Butler GJ. 2007. A combination of radiotherapy, nitric oxide and a hyperoxygenation sensitizing protocol for brain malignant tumor treatment. Medical Hypotheses 68:528–537.

Chougule PB, Akhtar MS, Akerley W, Ready N, Safran H, McRae R, Nigri P, Bellino J, Koness J, Radie-Keane K, et al. 1999. Chemoradiotherapy for advanced inoperable head and neck cancer: A phase II study. Seminars in Radiation Oncology 9(2 Suppl. 1):58–63.

Culot M, Lundquist S, Vanuxeem D, Nion S, Landry C, Delplace Y, Dehouck MP, Berezowski V, Fenart L, Cecchelli R. 2008. An in vitro blood–brain barrier model for high throughput (HTS) toxicological screening. Toxicology In Vitro 22:799–811.

Rump AF, Siekmann U, Kalff G. 1999. Effects of hyperbaric and hyperoxic conditions on the disposition of drugs: Theoretical considerations and a review of the literature. General Pharmacology 32:127–133.

Suzuki Y, Tanaka K, Shimizu M, Yoshida Y, Hashimoto T, Yamazaki H. 2008. Prediction of efficacy for malignant gliomas treated with carboplatin by pharmacokinetic parameters in combination with hyperbaric oxygenation. Neurologia medico-chirurgica, In Press.

Tanaka K, Yoshida Y, Hashimoto T, Gamura S, Shimizu M, Aoyama T, Yamazaki H. 2005. Pharmacokinetics of anti-cancer drug with hyperbaric oxygenation therapy. Neuro-Oncology 15:7–10 [in Japanese].

Tanaka K, Yoshida Y, Hashimoto T, Suga M, Yoshida K. 2004. Statistical study of chemotherapy for malignant gliomas. Neuro-Oncology 14:15–18 [in Japanese].

Yamazaki H, Shimizu M, Murayama N, Tanaka K, Nion S, Cecchelli R. 2008. Increased transendothelial permeability of anti-cancer agent carboplatin with aid of hyperbaric oxygenation. Xenobiotica 38:1298–1304.

Yamazaki H, Tanaka K, Gamura S, Hashimoto T, Shimizu M. 2006. High-performance liquid chromatographic assay for carboplatin in ultrafiltered plasma combined with hyperbaric oxygenation. Drug Metabolism and Pharmacokinetics 21:429–431.

Xenobiotica, October 2008; 38(10): 1298–1304

Increased transendothelial permeability of anti-cancer agent carboplatin with the aid of hyperbaric oxygenation

H. YAMAZAKI[1], M. SHIMIZU[1], N. MURAYAMA[1], K. TANAKA[2], S. NION[3], & R. CECCHELLI[4]

[1]*Laboratory of Drug Metabolism and Pharmacokinetics, Showa Pharmaceutical University, Machida, Japan,* [2]*St. Marianna University School of Medicine, Kawasaki, Japan,* [3]*CELLIAL Technologies, Lens, France, and* [4]*Université d'Artois, Lens, France*

(*Received 7 June 2008; revised 10 August 2008; accepted 13 August 2008*)

Abstract

1. The objective was to investigate the transport of an anticancer agent carboplatin across the blood–brain barrier in combination with hyperbaric oxygenation treatment. An *in vitro* well-validated model of bovine brain capillary endothelial cells was used.
2. A transendothelial transport of doxorubicin, a known P-glycoprotein substrate, was enhanced 1.5-fold by verapamil for 2-h incubation at 37°C. A transendothelial permeability coefficient of carboplatin (1.29×10^{-3} cm min^{-1}) was also increased 1.8-fold by verapamil.
3. Under the hyperbaric oxygenation conditions (at 0.2 MPa for the first 10 min), the transendothelial transport for 2 h of doxorubicin and carboplatin were increased 1.3- to 1.8-fold by hyperbaric oxygenation, like the suppressive effects of verapamil on P-gp function, without increase of the transport of lucifer yellow, a non P-glycoprotein substrate.
4. Combination of hyperbaric oxygenation treatment and verapamil could not further increase the permeability coefficients of these drugs that were already enhanced by either treatment, implying the P-glycoprotein-mediated carboplatin efflux transport similarly as doxorubicin.
5. Together with our reported high efficacy of carboplatin combined with hyperbaric oxygenation therapy on brain tumours, the present results suggest that carboplatin could be transported by P-glycoprotein, but that this efflux mechanism would be reduced by the hyperbaric oxygenation with the consequences of clinical efficacy.

Keywords: *Anti-cancer drug, brain, carboplatin, hyperbaric oxygenation, transport*

Correspondence: H. Yamazaki, Showa Pharmaceutical University, Laboratory of Drug Metabolism and Pharmacokinetics, Machida, Tokyo 194-8543, Japan. E-mail: hyamazak@ac.shoyaku.ac.jp

ISSN 0049-8254 print/ISSN 1366-5928 online
DOI: 10.1080/00498250802405472

Introduction

Toxicity to the central nervous system is a key issue in early safety assessment of compounds (Crofton et al. 2004). The P-glycoprotein (P-gp) pump, a member of the ATP-binding cassette superfamily of drug transporters (Sarkadi et al. 1992), is responsible for limiting entry of drugs into the central nervous system. On the contrary, resistance of tumour cells to a variety of drugs is a serious problem in cancer chemotherapy (Gottesman and Pastan 1993). Carboplatin (*cis*-diammine-1,1-cyclobutanedicarboxylatoplatinum(II)) is a second-generation platinum antineoplastic agent with clinical efficacy including modest activity against brain tumours (Allen et al. 1987). Recently, we obtained high efficacy of carboplatin combined with hyperbaric oxygenation (HBO) therapy on brain tumours at St. Marianna University School of Medicine Hospital (Tanaka et al. 2004, 2005; Yamazaki et al. 2006), in a similar manner using reported cellular systems (Kalns et al. 1998). HBO therapy has been generally used to treat a decompression sickness, variety of infections and ischaemic damages (Chougule et al. 1999). However, the detailed mechanism of improved clinical efficacy of medicines including carboplatin with the HBO therapy is unknown. To explain these novel findings, investigations for mechanisms of carboplatin transports across the blood–brain barrier and their modulation with HBO would be needed.

In the present study we investigated the carboplatin transfer across an *in vitro* model of the blood–brain barrier (Cecchelli et al. 1999; Culot et al. 2008), which could mimic *in vivo* condition. P-glycoprotein is clearly shown to be expressed in this blood–brain barrier model (Cecchelli et al. 1999; Culot et al. 2008). We reported herein the P-gp-mediated efflux transports of carboplatin and doxorubicin could be suppressed by HBO in the blood–brain barrier model. Clinical efficacy would be expected in consequence of enhanced transendothelial permeability of anti-cancer agents with hyperbaric oxygenation.

Materials and methods

Chemicals

Carboplatin (molecular weight = 371.25) was obtained from Bristol-Myers (Tokyo, Japan). Doxorubicin, verapamil, rhodamine 123, and lucifer yellow CH were purchased from Sigma-Aldrich (St Louis, MO, USA). All other chemicals were of the highest quality commercially available.

In vitro *blood–brain barrier model and insect microsomes expressing P-gp*

The *in vitro* blood–brain barrier model (Cecchelli et al. 1999; Culot et al. 2008) (CT Bovial-screen pack) was obtained from Nosan (Yokohama, Japan). The general procedures to prepare *in vitro* blood–brain barrier model with this kit were described previously (Cecchelli et al. 1999; Culot et al. 2008). Briefly, rat glial cells were cultured on a six-well plate in Dulbecco's modified eagle medium supplemented with 10% (v/v) foetal calf serum (Hyclone Laboratories, Logan, UT, USA), 2 mM glutamine, and 50 $\mu g\,ml^{-1}$ of gentamicin for 3 weeks. Bovine endothelial cells were separately cultured on two 60-mm diameter gelatin-coated Pétri dishes. Polycarbonate filters (Millicell-PC, 3 μm pore size, 30 mm; Millipore Corporation, Carrigtwahill, Cork, Ireland) were coated on the upper side with rat tail collagen prepared by a modification of the method (Dehouck et al. 1990). Confluent endothelial cells were trypsinized and plated on the upper side of the filter at a concentration

of 4×10^5 cells ml^{-1}. Inserts were placed on glial cell cultures and co-cultured in Dulbecco's modified eagle medium supplemented with 10% (v/v) calf serum, 10% (v/v) horse serum, 2 mM glutamine, 50 $\mu g\,ml^{-1}$ of gentamicin and 1 $ng\,ml^{-1}$ of basic fibroblast growth fact. The endothelial cells formed a confluent monolayer and presented the blood–brain barrier characteristics after 12 days (Cecchelli et al. 1999; Culot et al. 2008).

Insect microsomes expressing human P-gp for vanadate-sensitive ATPase assay were obtained from GenoMembrane (Yokohama, Japan). Inorganic phosphate generated by ATP hydrolysis linked with ABC transporters (Sarkadi et al. 1992) was determined by colorimetry according to the manufacturer's protocol.

Transendothelial transport experiments

Before the transport experiments, Ringer–Hepes buffer solution (pH 7.4) was added to empty wells of six-well plates (2.5 ml per well; Millipore, Billerica, MA, USA). Filter inserts, with or without confluent monolayers of bovine brain capillary endothelial cells, were subsequently placed in six-well plates. The test compound and/or verapamil (25 μM) and the integrity marker of the blood–brain barrier (20 μM of lucifer yellow) in water or dimethyl sulfoxide (DMSO) were added to the cell monolayer (1.5 ml). In the cases of HBO treatment, the plates were introduced to a hyperbaric oxygen chamber for small animals (Model P-5100S, Barotec Hanyuda, Tokyo, Japan) connected with a gas cylinder containing 50% O_2 and 50% N_2 at 0.2 MPa for 10 min (increase or decrease of atmosphere for 5 min) in a room held at constant temperature (37°C). Then the plates were placed on an orbital shaker at 37°C for transport experiments under the normal conditions.

Aliquots (200 μl) from the donor solution were taken at the beginning and at the end of 120-min incubation. Ultra-filtrate samples containing carboplatin obtained from *in vitro* blood–brain barrier models were analysed by the high-performance liquid chromatography system described previously (Yamazaki et al. 2006). Doxorubicin in the media were determined by high-performance liquid chromatography (Zhao and Dash 1999). The amounts of fluorescent tracer (lucifer yellow) in samples (200 μl) were determined fluorimetrically at the excitation wavelength of 420 nm and the emission wavelength of 535 nm with a microplate reader (TriStar LB 941, Berthold, Bad Wildbad, Germany).

Data analysis and calculation

The linearity of permeability was confirmed in controls and experiments in exactly the same conditions for 2 h. The cleared volume was calculated by dividing the amount of compound in the receiver compartment by the drug concentration in the donor compartment as described previously (Cecchelli et al. 1999; Culot et al. 2008). The slope of the clearance curve with inserts alone (free) and inserts with cells (tissue) is equal to PS_f and PS_t, respectively, where PS is the permeability–surface area product. The units of PS and S are in $\mu l\,min^{-1}$ and cm^2, respectively. The PS value for the endothelial monolayer (PS_e) was computed as follows (Cecchelli et al. 1999; Culot et al. 2008):

$$1/PS_e = 1/PS_t - 1/PS_f.$$

To generate the endothelial permeability coefficient, P_e (cm min^{-1}), the PS_e value was divided by the surface area of the insert (4.2 cm^2 for Millicell-PC). To assess possible adsorption to plastics or non-specific binding to cells, the mass balance (%) was calculated

from the amount of compound recovered in both compartments at the end of the experiment divided by the total amount added in the donor compartment at 0 min (Cecchelli et al. 1999; Culot et al. 2008).

All statistical analyses were carried out with the InStat program (GraphPad Software, San Diego, CA, USA).

Results and discussion

Since P-gp is of key importance for the functional blood–brain barrier model, its activity was assessed in the present *in vitro* model by measuring the uptake of rhodamine 123 (20 μM, a selective substrate of P-gp), before anti-cancer drug transport experiments. The permeability coefficient values of rhodamine 123 were determined to be 1.04 ± 0.15 and 1.79 ± 0.45 (10^{-3} cm min^{-1}, mean and SD, $n = 3$), respectively, in the absence and presence of a typical P-gp inhibitor, verapamil. Under the present condition, the similar monolayer integrity was confirmed by the permeability coefficient values ($<1.0 \times 10^{-3}$ cm min^{-1}) of the co-incubated lucifer yellow in the absence and presence of verapamil.

After the confirmation of suitability for transendothelial transport experiments, concentrations of anticancer drugs in the donor and acceptor compartments in the model were determined in cell-free and endothelial cell systems. As shown in Table I, in the cell-free system approximately one-third of the added substrate concentrations were detected in the receiver compartments after 2-h incubation. The transport of doxorubicin, a known substrate of P-gp, was apparently increased by verapamil in the endothelial cells under the atmosphere of HBO conditions. Similar results were seen in the carboplatin transport in this model at substrate concentrations of 2.5 and 50 μM as in the case of doxorubicin.

From these drug concentrations, a permeability coefficient of each substance was calculated (Table I). Under all conditions, no changes of the monolayer integrity were checked using co-incubated marker lucifer yellow. The transendothelial permeability coefficient of doxorubicin determined at a substrate concentration of 10 μM was calculated to be 0.65×10^{-3} cm min^{-1} under the control conditions. This transendothelial permeability coefficient value of doxorubicin was increased by addition of verapamil to the cells (1.5-fold) or under the HBO condition (1.3-fold). The transendothelial permeability coefficient of carboplatin determined at 50 μM were 1.29×10^{-3} cm min^{-1} under the atmosphere. The transendothelial permeability coefficient of carboplatin was significantly increased by verapamil (1.8-fold) or under HBO treatment (1.8-fold). Combinations of addition of verapamil and HBO treatment could not further significantly enhance the transendothelial permeability coefficients of doxorubicin and carboplatin, implying the saturations of the modifiers on the P-gp function. These results suggested that carboplatin efflux could be mediated by P-gp in the similar manner of doxorubicin and that the function of P-gp in the blood–brain barrier might be reduced by the HBO conditions.

To investigate further the effects of HBO on the relationship between P-gp and carboplatin, ATPase activities of recombinant P-gp were also determined. However, as shown in Table II, the activities obtained from vanadate-sensitive ATPase assays seemed to indicate little interaction between P-gp and carboplatin and undetectable effects of carboplatin on the verapamil-mediated ATPase activity of P-gp. The modulation of the P-gp function by HBO could not be determined in the present ATP assay systems, presumably because of one of false-negative cases (Sarkadi et al. 1992).

Table I. Doxorubicin and carboplatin transport across the blood–brain barrier in the absence or presence of the endothelial cells under the atmosphere and hyperbaric oxygenation (HBO) conditions.

			Abluminal concentration[a] (μM)		P_e (10^{-3} cm min^{-1})[b]		BBB integrity[c]	
Compound	Conditions	Endothelial cells	Without verapamil	With verapamil, 25 μM	Without verapamil	With verapamil	Without verapamil	With verapamil
Doxorubicin,	Control	−	3.35 ± 0.16 (100)	3.45 ± 0.01 (103)	−	−	−	−
10 μM		+	2.06 ± 0.15 (61)	2.70 ± 0.06 (81)	0.65 ± 0.08 (100)	0.99 ± 0.07 (152)*	0.63 ± 0.15	0.67 ± 0.01
	HBO[d]	−	3.23 ± 0.19 (96)	3.28 ± 0.19 (98)	−	−	−	−
		+	2.23 ± 0.05 (67)	2.67 ± 0.11 (80)	0.86 ± 0.04 (132)*	0.95 ± 0.10 (146)*	0.46 ± 0.02	0.54 ± 0.12
Carboplain,	Control	−	0.83 ± 0.06 (100)	0.83 ± 0.06 (100)	−	−	−	−
2.5 μM		+	0.27 ± 0.08 (33)	0.36 ± 0.03 (43)	0.76 ± 0.30 (100)	1.27 ± 0.16 (167)	0.74 ± 0.11	0.95 ± 0.12
50 μM	Control	−	12.7 ± 0.1 (100)	12.1 ± 0.7 (95)	−	−	−	−
		+	7.1 ± 1.4 (56)	9.1 ± 1.3 (72)	1.29 ± 0.39 (100)	2.30 ± 0.49 (178)*	0.64 ± 0.02	0.82 ± 0.15
	HBO	−	10.9 ± 0.3 (86)	10.9 ± 0.3 (86)	−	−	−	−
		+	8.7 ± 0.5 (69)	9.0 ± 0.4 (71)	2.26 ± 0.47 (175)*	2.91 ± 0.34 (226)*	0.82 ± 0.06	1.01 ± 0.11
None (DMSO)	Control	+	−	−	−	−	0.84 ± 0.02	−
	HBO	+	−	−	−	−	0.85 ± 0.06	−

[a]Drug concentrations in abluminal compartments (total volume of 2.5 ml) were measured after incubation of substrates in luminal compartments (1.5 ml) for 2 h at 37°C in triplicate or quadruplicate determinations (mean ± standard deviation (SD)). Drug concentrations in luminal compartments were also checked for conformations of mass balance. Numbers in parentheses are a percentage of control.
[b]Endothelial permeability coefficient. *$p < 0.05$, one-way analysis of variance (ANOVA) followed by Dunnet's multiple comparison tests.
[c]Monolayer integrity of the blood–brain barrier (BBB) was checked using P_e values (10^{-3} cm min^{-1}) of co-incubated lucifer yellow (20 μM).
[d]Hyperbaric oxygenation treatment (HBO, at 0.2 MPa for the first 10 min, increase or decrease of atmosphere for 5 min) was carried out after the addition of chemicals to the model.

Table II. Effects of carboplatin on vanadate-sensitive ATPase activities in recombinant P-glycoprotein (P-gp).

Carboplatin (μM)	Vanadate-sensitive ATPase activities (P_i nmol min^{-1} mg^{-1} protein)	
	Without verapamil	With verapamil, 50 μM
0	12 ± 1	42 ± 2
10	9 ± 1	43 ± 1
100	8 ± 1	44 ± 2
180	10 ± 1	45 ± 3

Insect microsomes expressing human P-gp (20 μg) were incubated for 30 min at 37°C in the absence or presence of verapamil and carboplatin. Data are the means and standard deviation (SD) of triplicate determinations.

It has been reviewed that a single exposure to hyperbaric or hyperoxic conditions would not seem to affect single-dose pharmacokinetics of drugs eliminated by the kidney and liver (Rump et al. 1999). On the contrary, it could be possible that oxygen-induced cerebral vasoconstriction would result in some modification of drug pharmacokinetics, presumably because of a variety of biochemical changes in the brain such as inactivation of intracellular systems or changes of blood flow rates (Al-Waili and Butler 2007). Although mechanisms of carboplatin transports across the blood–brain barrier had not previously been known, in our preliminary clinical study a possibility of prolonged biological residence time of carboplatin might be relevant to the efficacy with HBO therapy for malignant gliomas. We also preliminarily found that carboplatin could be uptaken into rat brains at the detectable levels by the aid of hyperbaric oxygenation. In the present study, carboplatin was classified as low endothelial permeability (around 1×10^{-3} cm min^{-1} of P_e) among the typical reported substances (Cecchelli et al. 1999; Culot et al. 2008). A major contribution of P-gp on the limited transendothelial permeability of carboplatin was also suggested as in the case of doxorubicin. However, other efflux pump(s) than P-gp restrictive to carboplatin transport could not be ruled out because of insignificant but apparent synergic action (175% and 226%) of hyperbaric oxygenation and a known board inhibitory effect of verapamil (Table I). In conclusions, taken together with the present results and these findings, P-gp mediated transendothelial transport of carboplatin might be reduced by the HBO treatment. The detailed mechanism of the modulation of P-gp function by oxygen would need to be clarified. Increased permeability of P-gp-dependent medicines by HBO may rapidly reach pharmacologically or toxicologically significant concentrations in the central nervous system. Assessment of suppression of P-gp-dependent efflux drug transports across the blood–brain barrier by oxygenation is of interest in pharmacological barrier research.

Acknowledgements

The authors thank Yannick Delplace of CELLIAL Technologies (Lens, France), Dr Hikaru Yabuuchi of GenoMembrane (Yokohama, Japan) and Dr Yu Suzuki, Daisuke Negishi, and Haruka Yamaguchi of their laboratory for their help. This study was supported in part by the Ministry of Education, Science, Sports and Culture of Japan, the Ministry of Health, Labor and Welfare of Japan.

References

Allen JC, Walker R, Luks E, Jennings M, Barfoot S, Tan C. 1987. Carboplatin and recurrent childhood brain tumors. Journal of Clinical Oncology 5:459–463.

Al-Waili NS, Butler GJ. 2007. A combination of radiotherapy, nitric oxide and a hyperoxygenation sensitizing protocol for brain malignant tumor treatment. Medical Hypotheses 68:528–537.

Cecchelli R, Dehouck B, Descamps L, Fenart L, Buee-Scherrer V, Duhem C, Lundquist S, Rentfel M, Torpier G, Dehouck MP. 1999. In vitro model for evaluating drug transport across the blood–brain barrier. Advanced Drug Delivery Reviews 36:165–178.

Chougule PB, Akhtar MS, Akerley W, Ready N, Safran H, McRae R, Nigri P, Bellino J, Koness J, Radie-Keane K, et al. 1999. Chemoradiotherapy for advanced inoperable head and neck cancer: A phase II study. Seminars in Radiation Oncology 9(2 Suppl. 1):58–63.

Crofton KM, Makris SL, Sette WF, Mendez E, Raffaele KC. 2004. A qualitative retrospective analysis of positive control data in developmental neurotoxicity studies. Neurotoxicology and Teratology 26:345–352.

Culot M, Lundquist S, Vanuxeem D, Nion S, Landry C, Delplace Y, Dehouck MP, Berezowski V, Fenart L, Cecchelli R. 2008. An in vitro blood–brain barrier model for high throughput (HTS) toxicological screening. Toxicology in Vitro 22:799–811.

Dehouck MP, Meresse S, Delorme P, Fruchart JC, Cecchelli R. 1990. An easier, reproducible, and mass-production method to study the blood–brain barrier in vitro. Journal of Neurochemistry 54:1798–1801.

Gottesman MM, Pastan I. 1993. Biochemistry of multidrug resistance mediated by the multidrug transporter. Annual Reviews of Biochemistry 62:385–427.

Kalns J, Krock L, Piepmeier Jr E. 1998. The effect of hyperbaric oxygen on growth and chemosensitivity of metastatic prostate cancer. Anticancer Research 18:363–367.

Rump AF, Siekmann U, Kalff G. 1999. Effects of hyperbaric and hyperoxic conditions on the disposition of drugs: Theoretical considerations and a review of the literature. General Pharmacology 32:127–133.

Sarkadi B, Price EM, Boucher RC, Germann UA, Scarborough GA. 1992. Expression of the human multidrug resistance cDNA in insect cells generates a high activity drug-stimulated membrane ATPase. Journal of Biological Chemistry 267:4854–4858.

Tanaka K, Yoshida Y, Hashimoto T, Gamura S, Shimizu M, Aoyama T, Yamazaki H. 2005. Pharmacokinetics of anti-cancer drug with hyperbaric oxygenation therapy. Neuro-Oncology 15:7–10. [in Japanese].

Tanaka K, Yoshida Y, Hashimoto T, Suga M, Yoshida K. 2004. Statistical study of chemotherapy for malignant gliomas. Neuro-Oncology 14:15–18. [in Japanese].

Yamazaki H, Tanaka K, Gamura S, Hashimoto T, Shimizu M. 2006. High-performance liquid chromatographic assay for carboplatin in ultrafiltered plasma combined with hyperbaric oxygenation. Drug Metabolism and Pharmacokinetics 21:429–431.

Zhao P, Dash AK. 1999. A simple HPLC method using a microbore column for the analysis of doxorubicin. Journal of Pharmaceutical and Biomedical Analysis 20:543–548.

EUROPEAN JOURNAL OF CANCER 44 (2008) 383–390

available at www.sciencedirect.com

ScienceDirect

journal homepage: www.ejconline.com

Pilot study of anti-angiogenic vaccine using fixed whole endothelium in patients with progressive malignancy after failure of conventional therapy

Yurai Okaji[a,b,], Nelson H. Tsuno[a,b], Minoru Tanaka[a,c], Satomi Yoneyama[b], Mika Matsuhashi[a], Joji Kitayama[b], Shinsuke Saito[b], Yutaka Nagura[a], Takeshi Tsuchiya[b], Jun Yamada[b], Junichiro Tanaka[b], Naoyuki Yoshikawa[a], Takeshi Nishikawa[b], Yasutaka Shuno[b], Tomoki Todo[c], Nobuhito Saito[c], Koki Takahashi[a], Hirokazu Nagawa[b]*

[a]*Department of Transfusion Medicine, The University of Tokyo, 7-3-1 Hongo, Bunkyo-ku, Tokyo 113-0033, Japan*
[b]*Department of Surgical Oncology, The University of Tokyo, 7-3-1 Hongo, Bunkyo-ku, Tokyo 113-0033, Japan*
[c]*Department of Neurosurgery, The University of Tokyo, 7-3-1 Hongo, Bunkyo-ku, Tokyo 113-0033, Japan*

ARTICLE INFO

Article history:
Received 3 September 2007
Received in revised form
16 October 2007
Accepted 22 October 2007
Available online 3 December 2007

Keywords:
Angiogenesis
Blood supply
Colorectal cancer
Endothelium
Malignant brain tumour
Immunotherapy
Vaccine

ABSTRACT

Vaccines targeting tumour angiogenesis were recently shown to inhibit tumour growth in animal models. However, there is still a lack of information about the clinical utility of anti-angiogenic vaccination. Therefore, here, we aimed to test the clinical effects of a vaccine using glutaraldehyde-fixed human umbilical vein endothelial cells (HUVECs). Six patients with recurrent malignant brain tumours and three patients with metastatic colorectal cancer received intradermal injections of 5×10^7 HUVECs/dose (in total 230 vaccinations). ELISA and flow cytometry revealed immunoglobulin response against HUVECs' membrane antigens. ELISPOT and chromium-release cytotoxicity assay revealed a specific cellular immune response against HUVECs, which were lysed in an effectors:targets ratio-dependent manner. Gadolinium-contrasted MRI showed partial or complete tumour responses in three malignant brain tumour patients. Except for a DTH-like skin reaction at the injection site, no adverse effect of vaccination could be observed. Our results suggest that the endothelial vaccine can overcome peripheral tolerance of self-angiogenic antigens in clinical settings, and therefore should be useful for adjuvant immunotherapy of cancer.

1. Introduction

Angiogenesis, the growth of new blood vessels, is essential for tumour growth and metastasis.[1–5] Whereas angiogenesis occurs minimally in normal adult tissues, it is intensive in developing tumours, enabling them to grow over the diameter of a few mm, the so called 'angiogenic limit'. Angiogenesis-associated antigens over-expressed on tumour endothelium are specific molecular addresses targeted by anti-angiogenic therapy.[6–10] Therapeutic damage of tumour endothelium activates the coagulation cascade, and consequently results in the obstruction of tumour vasculature, with hypoxia and shrinkage of tumours due to necrosis, whereas it does not affect blood supply in normal adult tissues.[11] As a result, cancer

* *Corresponding author*: Address: Department of Transfusion Medicine, The University of Tokyo, 7-3-1 Hongo, Bunkyo-ku, Tokyo 113-0033, Japan. Tel.: +81 3 3815 5411x35165; fax: +81 3 3816 2516.
E-mail address: okaji-tky@umin.ac.jp (Y. Okaji).
0959-8049/$ - see front matter © 2007 Elsevier Ltd. All rights reserved.
doi:10.1016/j.ejca.2007.10.018

patients coexist with small tumours that can neither grow nor metastasise, under the condition called 'tumour dormancy'[12] or 'cancer without disease'.[13]

Vaccines targeting tumour angiogenesis were recently shown by us and others to inhibit tumour growth in animal models.[14,15] However, there is still a lack of information about the clinical utility of anti-angiogenic vaccination. Therefore, here, we aimed to test the clinical effects of a vaccine using glutaraldehyde-fixed human umbilical vein endothelial cells (HUVECs).

2. Patients and methods

2.1. Eligibility criteria

Patients with a recurrent malignant brain tumour or a metastatic colorectal cancer, previously treated in our hospital, were eligible. Eligibility criteria were as follows: A progressive disease resistant to conventional therapy, as assessed by contrasted computer tomography (CT) or magnetic resonance imaging (MRI), and classified according to the Response Evaluation Criteria in Solid Tumours[16]; at least a 1 month period after finishing prior therapy; WHO performance status 0–3 (malignant brain tumours) or 0–2 (colorectal cancer); haemoglobin $\geqslant$8 g/dL; bilirubin $\leqslant$2.0 mg/dL; serum glutamic oxaloacetic transaminase $\leqslant$100 IU/L; serum glutamate pyruvate transaminase $\leqslant$100 IU/L; creatinine $\leqslant$2 mg/dL; blood urea nitrogen $\leqslant$30 mg/dL; creatinine clearance $\geqslant$90 ml/min; ejection fraction by echocardiography $\geqslant$70% and prothrombin time $\geqslant$70%. In addition, patients with a psychiatric disorder, extensive cachexia, multiple cancer types, active infection, autoimmune disease or myocardial ischaemia were excluded. The Institutional Review Board of the University of Tokyo approved this protocol. All patients provided written informed consent before enrolment on protocol, in accordance with the Declaration of Helsinki.

2.2. Study design

This single arm phase I study was carried out between August 2003 and August 2007 to assess the clinical utility of a vaccine using human umbilical vein endothelial cells (HUVECs). The enrolled patients were given intradermal injections of 5×10^7 HUVECs/dose, first month weekly, and then every 2 weeks. Immune response was evaluated by examining patients' peripheral blood mononuclear cells (PBMC) and sera, which were isolated monthly and frozen until being tested in immunological assays later at the same time. Tumour response was assessed monthly by contrasted computer tomography (CT) or magnetic resonance imaging (MRI) according to the Response Evaluation Criteria in Solid Tumours.[16] Adverse effects were evaluated by monitoring the patients according to the Common Toxicity Criteria.[17]

2.3. Vaccine preparation and quality control

HUVECs were isolated from healthy donors as described,[14] and cultured on 0.1% gelatin (w/v)-coated dishes in EC-SFM (Life Technologies, Grand Island, NY), according to the manufacturer's recommendations. Specific properties of angiogenic endothelium were confirmed by measuring the expression of CD31, CD51, CD105, CD146, and binding of UEA (Ulex europaeus) lectin by flow cytometry (FACSCalibur, BD Biosciences, San Chose, CA; antibody concentration was 5 μg/ml). Negative presence of endotoxin in the cell cultures was confirmed by Toxicolour test (Seikagaku Co., Tokyo, Japan). HUVECs of up to ten passages were harvested, and fixed with 0.025% glutaraldehyde (v/v) as described ,[14] and stored at −80 °C in single dose aliquots, containing 5×10^7 cells/ml physiological saline for injection.

2.4. Enzyme-linked immunosorbent assay (ELISA)

96-well immunoplates (NUNC, Roskilde, Denmark) were coated with 10 μg/ml HUVECs' membrane proteins overnight at 4 °C, and blocked with 1% BSA (w/v), for 2 h at 37 °C. Patients' sera, diluted 2×, were used in duplicates as the primary antibody, and horseradish peroxidase conjugate of anti-IgG (Zymed, San Francisco, CA), diluted 2000×, as the secondary antibody. Colour-development by ABTS (ICN, Aurora, OH) was followed by determining optical density (O.D.) at 405 nm. For negative control, wells coated with K-562 (ATCC, Manassas, VA) were used. IgG reactivity was expressed as the ratio to the values measured in the pre-vaccination samples that were considered 100%.

2.5. Isolation of patients' B cells and flow cytometry

Patients' PBMC were cultured first in the supernatant of B95-8 (cotton-top tamarine lymphocyte cell line secreting Epstein–Barr virus, obtained from Japanese Collection of Research Bioresources, and cultured in RPMI - 10%FCS) supplemented with 5 μg/ml CpG-B-DNA (HyCult Biotechnology, Uden, The Netherlands), 10 ng/ml IL-6 (Strathmann Biotec, Zurich, Switzerland) and 2 μg/ml membrane proteins of HUVECs for 1 week, and then in RPMI-1640 supplemented with 10% FCS (v/v), 10 ng/ml IL-6, and 1% antibiotic/antimycotic (v/v; at final concentration of 100 U/ml penicillin G, 100 μg/ml streptomycin sulphate and 250 ng/ml amphotericin B; Life Technologies) for 3 weeks. Specific phenotype of selectively immortalised B cells was confirmed by analysing their expression of CD19 (B cell marker) and CD138 (plasmatic cells marker) by flow cytometry (FACSCalibur, BD Biosciences).

The supernatants of B cell media were added in the amounts of 200 μl to 2×10^5 HUVECs for 30 min at 4 °C. The cells were washed two times, incubated with FITC-labelled antibodies against human IgM or IgG (Zymed), diluted 40×, for another 30 min at 4 °C. Finally, the cells were washed two times, and their fluorescence measured in the flow cytometer (FACSCalibur, BD Biosciences).

2.6. IFN-γ enzyme-linked immunospot (ELISPOT) assay

Human IFN-γ ELISPOT kit (BD Biosciences) was used for the detection of patients' PBMC secreting IFN-γ in the presence or absence of HUVEC membrane proteins, according to the manufacturer's recommendations. The numbers and areas of colour-developed IFN-γ immunospots were determined by

KS ELISPOT system (Carl Zeiss Microimaging, Goettingen, Germany). The results were expressed as % IFN-γ spots, calculated as the ratio to the values measured in the pre-vaccination samples that were considered 100%.

2.7. *Intracellular cytokine flow cytometry (CFC) assay*

Re-stimulated patients' PBMC were carefully removed from the immunoplates at the end of ELISPOT assays, cultured for another 6 h in a medium supplemented with 10 μg/ml Brefeldin A (Sigma, Saint Louis, MO), fixed with 3% paraformaldehyde (v/v), permeabilised with 0.5% Tween-20 (v/v), and stained with 5 μg/ml FITC-/PE-labelled monoclonal antibodies against IFN-γ and CD3 (BD Biosciences). % CD3(+)IFN-γ(+) cells were determined by flow cytometry (FACSCalibur, BD Biosciences), and expressed as the ratio to the values obtained in the pre-vaccination samples that were considered 100%.

2.8. *Cytotoxicity T lymphocyte (CTL) assay*

Patients' PBMC were used as effectors against HUVECs or K562 at effectors:targets ratios 100:1, 30:1 and 5:1, in a ^{51}Cr-release cytotoxicity assay as described,[14] with some modifications as follows. Medium used for re-activation culture was RPMI-1640 - 10% FCS (v/v) - 100 U/ml recombinant human IL-2 (Sigma) - 1% antibiotic/antimycotic (v/v). % specific lysis was calculated using the formula (experimental release – spontaneous release) / (maximum release – spontaneous release) × 100. The results were expressed as the ratio to the values of the pre-vaccination samples that were considered 100%.

3. Results

3.1. *Patient characteristics*

Nine patients with a progressive malignancy, i.e. six patients with a recurrent malignant brain tumour and three patients with a metastatic colorectal cancer (median age: 53 years, range: 43–68 years), were enrolled in this study.

3.2. *Properties of vaccine endothelium*

Human umbilical vein endothelial cells (HUVECs) were isolated from fresh umbilical cords, cultured with angiogenic stimulators, fixed, and used as vaccines (Fig. 1a). The cells expressed CD31, CD51, CD105 and CD146, as well as bound UEA lectin, suggesting they were angiogenic endothelium (Fig. 1b).

3.3. *Safety of vaccination*

The patients received intradermal injections of 5×10^7 HUVECs/dose in the vaccination protocol (Fig. 1c), in a total amount of 230 vaccinations (Table 1; median number of vaccinations: 26 doses, range: 8–50 doses; median vaccination period: 12 months, range: 3–24 months). Except for a DTH-like skin reaction at the injection site, no adverse effect could be observed (data not shown).

3.4. *Specific antibody response*

Specific antibodies against HUVECs' membrane antigens were detected in the sera of eight patients (Fig. 2a), and could also be detected in the culture media of patients' B cells (Fig. 2b–d).

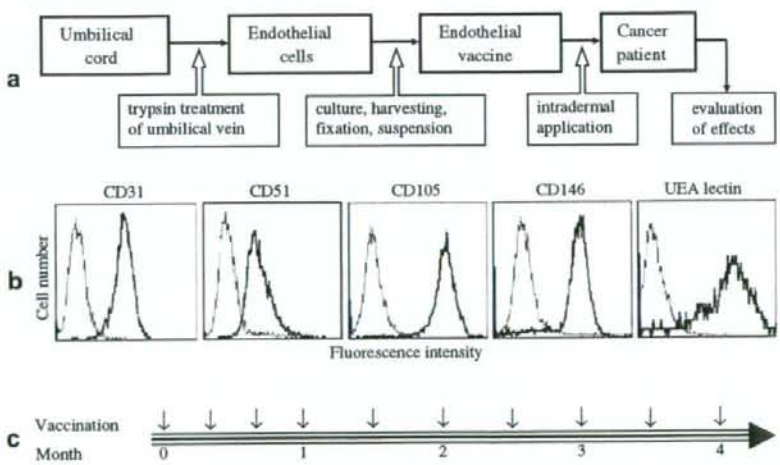

Fig. 1 – Study design. (a) Study protocol. Human umbilical vein endothelial cells (HUVECs) were isolated, cultured, harvested, fixed, and periodically injected in cancer patients. Vaccination effects, i.e. immune and tumour responses were evaluated monthly. (b) Confirmation of specific properties of HUVECs by flow cytometry. The cells expressed CD31, CD51, CD105 and CD146, as well as bound UEA lectin, suggesting they were angiogenic endothelium. (c) Vaccination protocol. The patients received vaccinations first month weekly, and then every 2 weeks.

Table 1 – Patients' characteristics and clinical response

#	Age/sex	Diagnosis	Prior therapy	Period	Doses	Ab	Cell	Response
1	47/F	PBMrec	sur, cht, xrt	24[a]	50[a]	+	+	PR
2	47/F	GBMrec	sur, cht, xrt	24[a]	50[a]	+	+	PR
3	48/F	AODrec	sur, cht, xrt	21[a]	44[a]	+	nd	CR
4	66/F	CRCmet	none	11	24	+	+	PD
5	54/M	GBMrec	sur, cht, xrt	8	18	+	+	PD
6	57/F	CRCmet	cht	7	16	+	+	PD
7	68/M	CRCmet	sur, cht, xrt	4	10	+	+	PD
8	46/M	GBMrec	sur, cht, xrt	4	10	+	nd	PD
9	43/F	AODrec	sur, cht, xrt	3	8	–	–	PD

Abbreviations: *M*, male; *F*, female; *PBMrec*, recurrent pinealoblastoma; *GBMrec*, recurrent glioblastoma multiforme; *AODrec*, recurrent anaplastic oligodendroglioma; *CRCmet*, metastatic colorectal cancer; *sur*, surgical therapy; *cht*, chemotherapy; *xrt*, radiation therapy; *Period*, vaccination period in months; *Doses*, number of vaccination doses; *Ab*, antibody response; *Cell*, cellular response; *nd*, not determined; *Response*, clinical tumour response; *PR*, partial response; *CR*, complete response; *PD*, progressive disease.
a Still in progress.

These antibodies reacted neither with non-endothelial control cells K-562 by ELISA and flow cytometry, nor with human leucocyte antigens of platelets pooled from multiple donors by mixed passive haemagglutination as described [18] (data not shown).

3.5. *Specific cellular response*

Increased secretion of IFN-γ as a response to the stimulation with HUVECs' membrane antigens was detected in six patients (Fig. 3a–c). Patients' cellular effectors specifically lysed HUVECs (Fig. 3d), but not K-562 (data not shown).

3.6. *Clinical tumour response*

Two partial and one complete tumour responses were observed on gadolinium contrasted MRI scans after 9 months of vaccination in three patients with recurrent malignant brain tumours (Fig. 4). In detail, in the patient #1 with pinealoblastoma, a recurrent disease accompanied by dissemination in the cerebrospinal fluid space that resulted in multiple new tumour lesions outside the post-operative radiation field (including one lesion being localised near the brain stem) was first detected 2 years after completed prior therapy. In the patient #2 with glioblastoma multiforme, and patient #3 with anaplastic oligodendroglioma, recurrences were first detected 9 and 20 months after completed prior therapy, respectively. Recurrent disease was treated first by chemotherapy with temozolomide, but without any effect, and therefore the patients were enrolled in the present study. After 9 months of subsequent endothelial vaccination, partial tumour responses lasting over 12 months were observed in the patients #1 and #2, and a complete tumour response lasting over 9 months was observed in the patient #3 (the protocol was still in progress at the time of manuscript preparation).

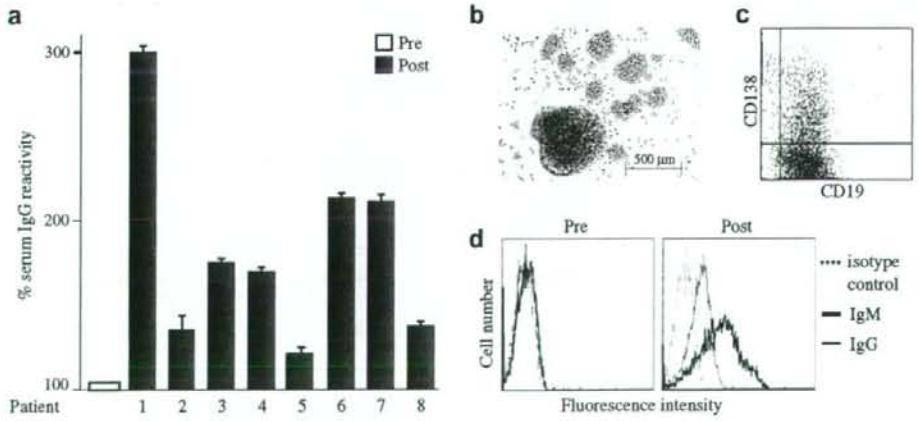

Fig. 2 – Specific antibody response. (a) Reactivity of patients' serum IgG with HUVECs' membrane antigens by enzyme-linked immunosorbent assay. Representative relative reactivities (Post/Pre) determined during best responses are shown. (b) Patients' peripheral blood B cells. Representative growing colonies of patient #1 B cells, selectively immortalised and cultured, are shown. (c) CD19 and CD138 expression on patient #1 B cells measured by flow cytometry. (d) Reactivity of IgM and IgG secreted by patient #1 B cells with HUVECs measured by flow cytometry.